LETTERS
PUBLISHED ONLINE: 31 JULY 2017 | DOI: 10.1038/NCLIMATE3350
nature climate change

A global framework for future costs and benefits of river-flood protection in urban areas

Philip J. Ward[1]*, Brenden Jongman[1,2], Jeroen C. J. H. Aerts[1], Paul D. Bates[3,4], Wouter J. W. Botzen[1,5], Andres Diaz Loaiza[1], Stephane Hallegatte[6], Jarl M. Kind[7], Jaap Kwadijk[8], Paolo Scussolini[1] and Hessel C. Winsemius[1,7]

Floods cause billions of dollars of damage each year[1], and flood risks are expected to increase due to socio-economic development, subsidence, and climate change[2–4]. Implementing additional flood risk management measures can limit losses, protecting people and livelihoods[5]. Whilst several models have been developed to assess global-scale river-flood risk[2,4,6–8], methods for evaluating flood risk management investments globally are lacking[9]. Here, we present a framework for assessing costs and benefits of structural flood protection measures in urban areas around the world. We demonstrate its use under different assumptions of current and future climate change and socio-economic development. Under these assumptions, investments in dykes may be economically attractive for reducing risk in large parts of the world, but not everywhere. In some regions, economically efficient investments could reduce future flood risk below today's levels, in spite of climate change and economic growth. We also demonstrate the sensitivity of the results to different assumptions and parameters. The framework can be used to identify regions where river-flood protection investments should be prioritized, or where other risk-reducing strategies should be emphasized.

Recently, a first generation of global river-flood risk models has been developed[2,4,6–8]. A limitation is their assumption that no flood protection infrastructure is in place, leading to overestimations of risk[6]. Several studies have assessed flood risk using simple assumptions of current protection standards[3,10,11]. However, they did not assess costs and benefits of further investments in increasing flood protection. This information is useful for planning investments in flood risk management and adaptation[12–14]. Here, we demonstrate a framework for cost–benefit analysis of flood risk reduction using the GLOFRIS[6,7] global flood risk model.

First, we used GLOFRIS[6,7] to calculate current river-flood risk in urban areas, with and without protection. Assumptions for current protection standards are from FLOPROS[15] (Supplementary Fig. 1), a database of sub-national scale protection standards. Globally, modelled Expected Annual Damage (EAD) is 91% lower when estimates of current protection standards are included ($94 billion versus $1031 billion). Therefore, current protection already provides large societal benefits (Fig. 1).

Since flood protection is not optimal today and risk will change over time, it may be desirable to increase protection standards in some regions. We explore three 'adaptation objectives'—that is, three approaches to developing risk reduction strategies through dykes. The 'optimize' objective prescribes protection standards that maximize Net Present Value (NPV). Since optimization studies are complex and rare in practice[13], we also test two simpler objectives. The 'constant absolute risk' objective keeps future EAD constant in absolute terms at current levels, assuming no change in societal preferences towards absolute risk. The 'constant relative risk' objective keeps future EAD as a percentage of Gross Domestic Product (GDP) constant, reflecting a desire to keep flood risk constant as a share of the economy.

Aggregated globally, modelled Benefit:Cost (B:C) ratios exceed 1 for all objectives for the scenarios shown in Table 1. The only exception is RCP6.0/SSP3, for 'constant absolute risk'. Results shown here are averaged across five global climate models (GCMs), using a 5% per year discount rate and middle-estimate investment costs (Methods). The four scenarios shown represent plausible combinations of Representative Concentration Pathways[16] (RCPs) and Shared Socioeconomic Pathways[17] (SSPs). The scenario selection is described in Supplementary Information 1. Other RCP/SSP combinations are plausible, so Supplementary Table 1 shows results for all combinations.

By definition, highest NPVs are achieved under the 'optimize' objective. Global costs are lowest for 'optimize', and highest for 'constant absolute risk'. For the latter, NPV is on average 61% lower than for 'optimize' (range: 16–138% lower), whilst for 'constant relative risk', NPV is on average 35% lower than for 'optimize' (range: 15–69% lower). Given the high B:C ratios, even if the 'optimize' objective is not pursued, the simpler objectives are preferable to doing nothing. RCP8.5/SSP5 would entail higher investments than if more stringent international climate policies achieve lower greenhouse gas concentrations (Table 1). Sensitivity analysis was carried out using 3% and 8% per year discount rates (Supplementary Table 2); only for RCP8.5/SSP5 do we see B:C ratios under 1 (for 'constant absolute risk' and 'constant relative risk' and 8% discount rate).

Protection standards required per sub-national unit to achieve the 'optimize' objective are shown in Fig. 2, with associated B:C ratios in Supplementary Fig. 2. For large parts of North America, Australia, northern Europe, and East Asia, these optimal standards could decrease future absolute EAD (in 2080) below current values (Supplementary Fig. 3). However, for most of the world, their implementation would still lead to overall increases in absolute EAD.

Nevertheless, the optimal standards would lead to decreases in future EAD as a percentage of GDP, in large parts of the world (Supplementary Fig. 4). This is particularly the case for the aforementioned regions, and for South Asia, Europe, and Central

[1]Institute for Environmental Studies (IVM), Vrije Universiteit Amsterdam, 1081 HV Amsterdam, the Netherlands. [2]Global Facility for Disaster Reduction and Recovery, The World Bank Group, Washington DC 20433, USA. [3]University of Bristol, Bristol BS8 1TH, UK. [4]SSBN Flood Risk Solutions, Bristol BS1 6QH, UK. [5]Utrecht University School of Economics (U.S.E.), Utrecht University, 3508 TC Utrecht, the Netherlands. [6]The World Bank, Washington DC 20433, USA. [7]Deltares, Delft/Utrecht, 2600 MH Delft, the Netherlands. [8]Twente University, 7500AE Enschede, the Netherlands. *e-mail: philip.ward@vu.nl

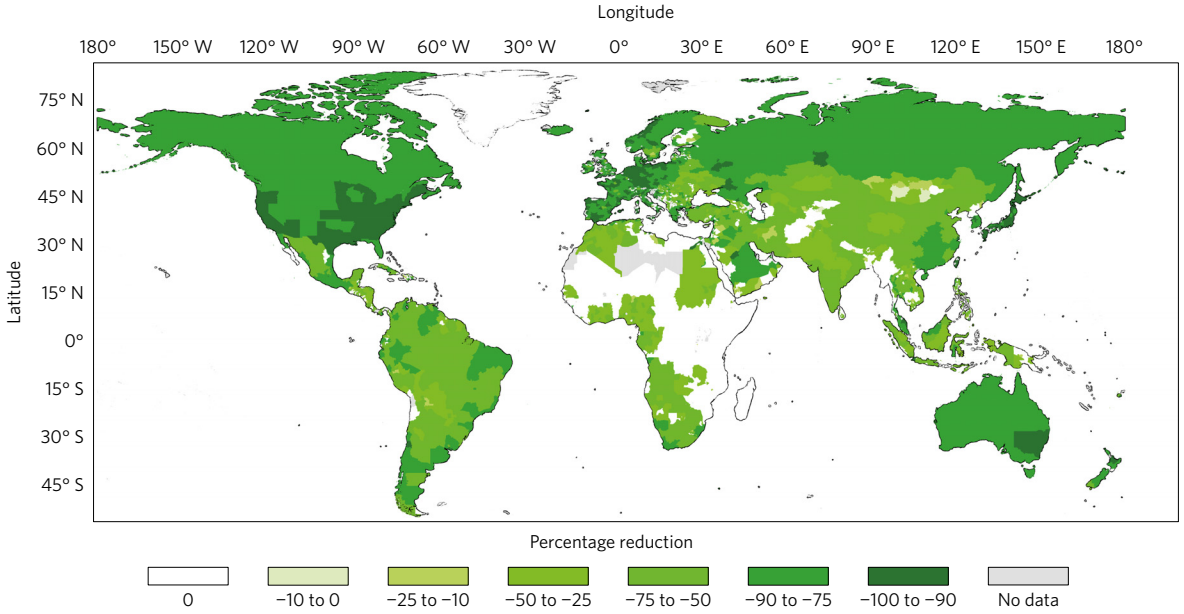

Figure 1 | Percentage reduction in current expected annual damage for simulations carried out with assumed current protection standards compared to no flood protection.

Table 1 | Globally aggregated results for the 'optimize', 'constant absolute risk', and 'constant relative risk' adaptation objectives.

Adaptation objectives	Scenario			
	RCP2.6/SSP1	RCP4.5/SSP2	RCP6.0/SSP3	RCP8.5/SSP5
Objective: optimize				
Benefits (US$ billion per year)	316	254	105	799
Costs (US$ billion per year)	47	44	27	78
Benefit:Cost ratio	6.7	5.7	3.9	10.2
NPV (US$ billion per year)	269	210	78	721
Objective: constant absolute risk				
Benefits (US$ billion per year)	339	276	125	827
Costs (US$ billion per year)	170	177	155	219
Benefit:Cost ratio	2.0	1.6	0.8	3.8
NPV (US$ billion per year)	169	99	−30	608
Objective: constant relative risk				
Benefits (US$ billion per year)	275	225	100	721
Costs (US$ billion per year)	73	80	76	108
Benefit:Cost ratio	3.8	2.8	1.3	6.7
NPV (US$ billion per year)	202	145	24	613

The table shows the average results across the five Global Climate Models, under the following assumptions: middle-estimate investment costs; maintenance costs of 1% per year; and a discount rate of 5% per year. We assumed that the construction of dykes begins in 2020 and is completed by 2050, and that by 2050 dykes are designed to the standard required for the climate at the end of the twenty-first century (2060–2099). Annual costs are based on the period 2020–2100.

Africa. In the latter regions, flood risk would increase, but slower than economic growth. Even though our simulations found no protection standards with positive NPV in many parts of South America, EAD relative to GDP decreases by 2080 in large parts of southwestern South America. Here, projected economic growth is greater than projected increases in absolute flood risk.

For individual GCMs, Supplementary Figs 5 and 6 show that whilst there are differences between GCMs in terms of optimal protection standards and B:C ratios, the overall regional patterns are robust in terms of where benefits of additional dykes outweigh costs. This pattern is consistent at 3% and 8% discount rates (Supplementary Figs 7 and 8). For the low-cost estimate (Supplementary Fig. 9), positive NPVs are achieved for the 'optimize' objective in most regions, including many parts of South America and Africa. For the high-cost estimate (Supplementary Fig. 10), the general spatial pattern remains, albeit with lower protection standards and fewer sub-national units where positive NPVs are achieved.

B:C ratios per sub-national unit for 'constant absolute risk' and 'constant relative risk' are shown in Fig. 3a,b respectively, for RCP4.5/SSP2. Results for the other scenarios can be found in Supplementary Figs 11 and 12, respectively, and corresponding protection standards in Supplementary Figs 13 and 14. Whilst future absolute risk could theoretically be contained at today's levels, Fig. 3a shows that doing this with dykes would be economically undesirable in those areas with B:C ratios less than 1. Generally, B:C ratios are higher for 'constant relative risk' (Fig. 3b), although the overall spatial pattern is similar. Since future hydrological simulations are sensitive to the choice of GCM and scenario[18], Fig. 3c,d shows the percentage of simulations (over all combinations of five GCMs and four RCP/SSPs discussed) for which the B:C ratio exceeds 1. Such information is useful, since it identifies regions with high agreement between models and scenarios, where investments could be prioritized. The overall spatial pattern is robust using 3% and 8% per year discount rates (Supplementary Figs 15 and 16).

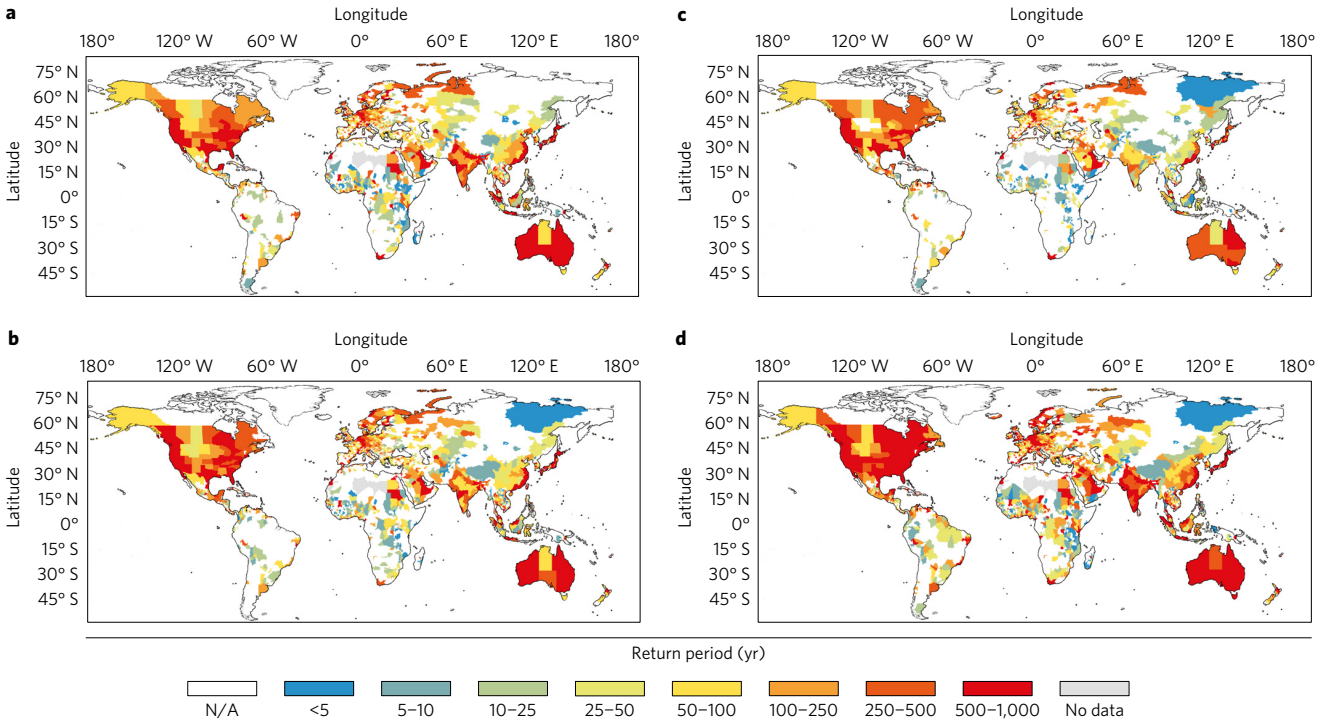

Figure 2 | Protection standards at sub-national level in 2080 that meet the 'optimize' objective. a–d, The average return period is shown across the five GCMs, for: RCP2.6/SSP1 (**a**); RCP4.5/SSP2 (**b**); RCP6.0/SSP3 (**c**); and RCP8.5/SSP5 (**d**). Sub-national units in which no increase in protection standard provides a positive NPV are indicated by N/A. Results are shown assuming middle-estimate investment costs, maintenance costs of 1% per year, and a discount rate of 5% per year.

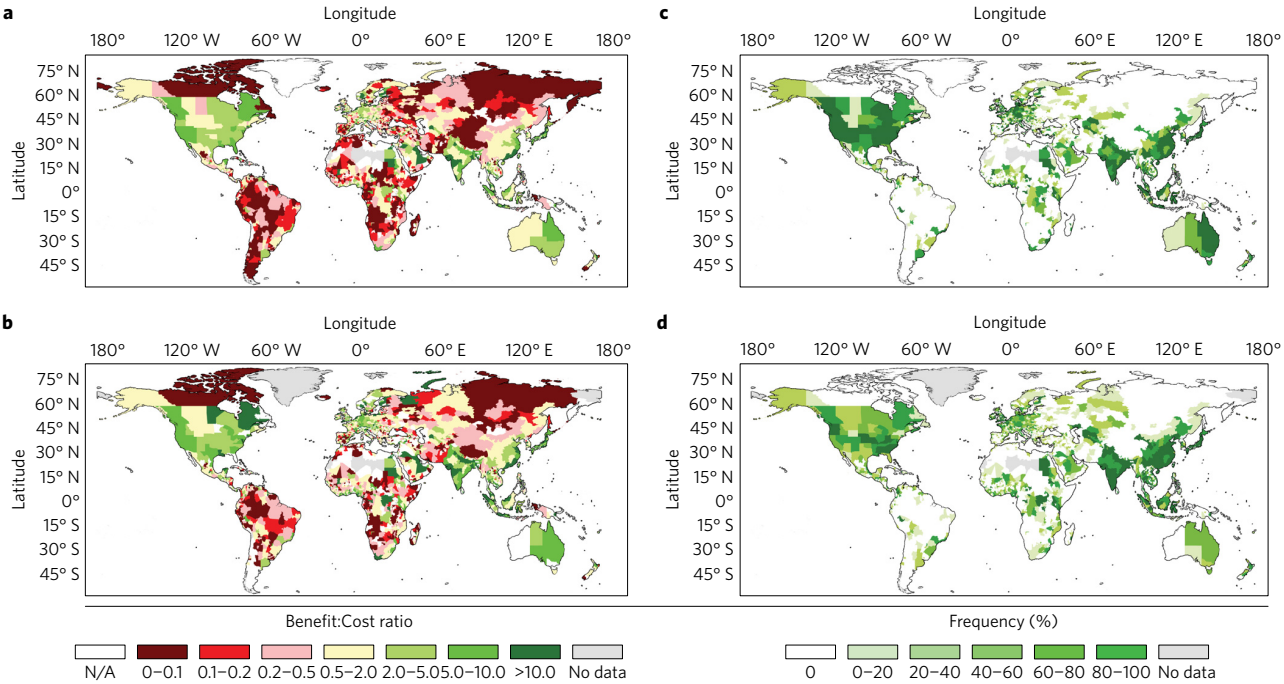

Figure 3 | B:C ratio at sub-national level, and percentage of models for which B:C ratio exceeds 1, for the EAD-constant and EAD/GDP-constant adaptation objections. a,**b**, B:C ratio for the following adaptation objectives: EAD-constant (**a**,**c**) and EAD/GDP-constant (**b**,**d**). **c**,**d**, B:C ratio exceeding 1, as a percentage of the simulations for all five GCMs and the following four RCP/SSP combinations: RCP2.6/SSP1; RCP4.5/SSP2; RCP6.0/SSP3; and RCP8.5/SSP5 (that is, $n = 20$). Results are shown here assuming middle-estimate investment costs, maintenance costs of 1% per year, and a discount rate of 5% per year.

Given the large number of assumptions used, we examine in detail the sensitivity of the results to different: RCP/SSPs; GCMs; discount rates; cost estimates; and baseline protection standards. Results for all assumptions are described in Supplementary Information 2 and made available in the Supplementary Data Set. An important uncertainty stems from the estimates of current flood protection standards from FLOPROS (Methods). The framework allows this standard to be changed, when better information is

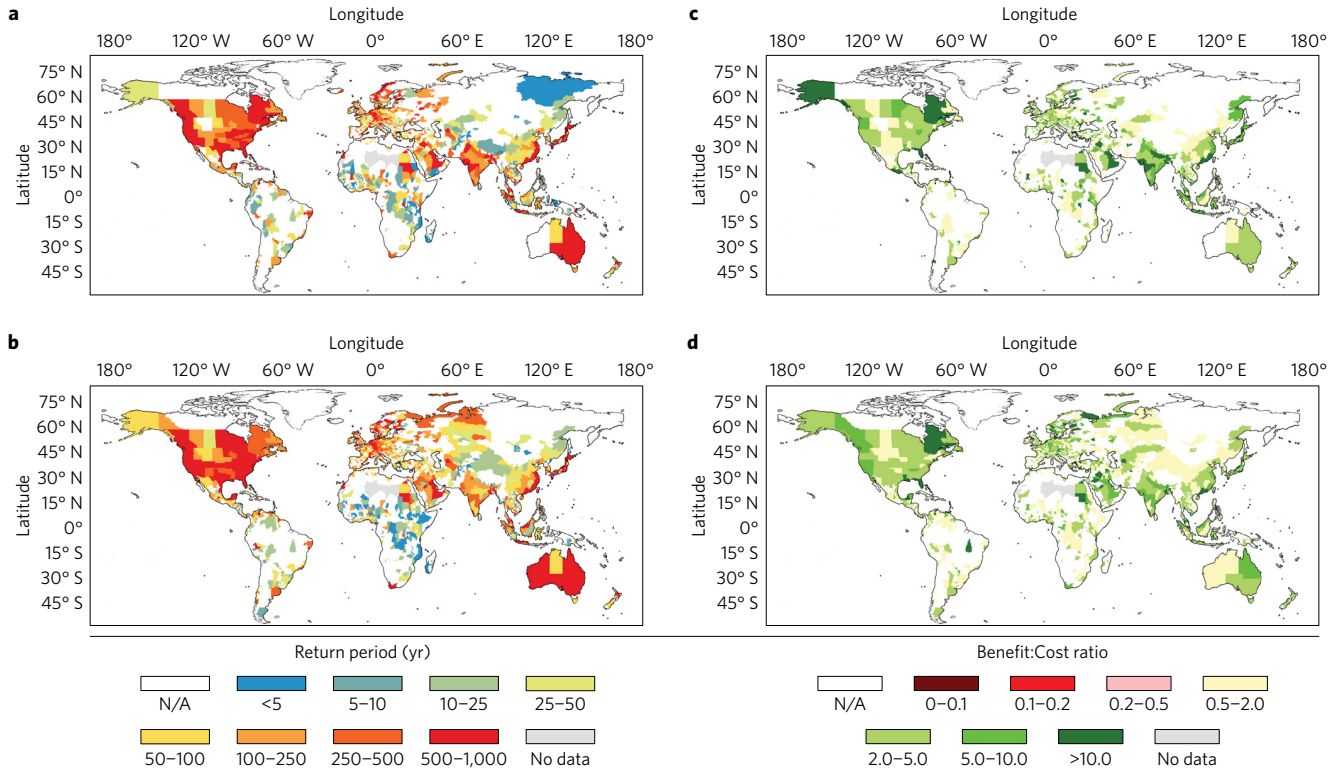

Figure 4 | Protection standards at sub-national level in 2080 and associated B:C ratios. a,**b**, Protection standards that meet the 'optimize' objective. **c**,**d**, B:C ratios associated with **a**,**b**, respectively. The simulations are used to show the robustness of the results (in terms of simulated protection standards and B:C ratios) across the different combinations of RCPs/SSPs, estimates of investment costs, and discount rates. **a** and **c** are based on the low estimates of investments costs, a discount rate of 3% per year, and RCP8.5/SSP5. This combination represents the highest B:C ratio at the globally aggregated scale. **b** and **d** are based on the high estimates of investments costs, a discount rate of 8% per year, and RCP2.6/SSP3. This combination represents the lowest B:C ratio at the globally aggregated scale.

available from users. We test the sensitivity of results to this assumption by also carrying out simulations assuming current flood protection to be: half that in FLOPROS (Supplementary Figs 17 and 18 and Supplementary Table 3); and double that in FLOPROS (Supplementary Figs 19 and 20 and Supplementary Table 4). The results are robust in terms of their influence on the B:C ratio and the order of magnitude of the optimal flood protection standard.

We also assess the robustness of the results to the various assumptions. In Fig. 4, we show protection standards and B:C ratios for two simulations—under the 'optimize' objective—at either end of the parameter spectrum. We selected RCP/SSP combinations providing the highest (RCP8.5/SSP5) and lowest (RCP2.6/SSP3) B:C ratios. We combined RCP8.5/SSP5 with low-cost estimates and a 3% per year discount rate (panels a,c). We combined RCP2.6/SSP3 with high-cost estimates and an 8% per year discount rate (panels b,d). Globally, these represent the simulations with the highest and lowest benefits relative to costs, respectively. Whilst values for benefits and costs are different, Fig. 4 shows the overall spatial patterns in B:C ratios and protection standards to be consistent. In Supplementary Information 2.6 we discuss overall robustness; Supplementary Fig. 21 shows the percentage of simulations in which the B:C ratio exceeds 1 across all 2,700 combinations of parameters discussed in this paper, showing the conclusions to be very robust in many regions.

In this paper, we used the GLOFRIS inundation model, which uses a volume-spreading algorithm, rather than a hydrodynamic scheme. More complex hydrodynamic models can potentially simulate present-day inundation more accurately[19]. However, of the six models used in a recent comparison study of global flood models[20], GLOFRIS is the only one that has been used to simulate high-resolution inundation under future climate scenarios. For two of the other models, the use of regional flood frequency curves instead of climate input data means that future simulations cannot be performed in the current setup. For the other models, long runtimes have meant that any future simulations have been carried out only at lower resolution, or on the discharge component only. We tested whether GLOFRIS is able to simulate inundation with high enough skill in urban areas so that the flood impact results do not deviate excessively from impact results based on more accurate inundation maps. To do this, we carried out the most extensive benchmarking experiment to date of global model results compared to local data (Supplementary Information 3). For eight case studies, we compared GLOFRIS inundation maps with inundation maps from local models or satellite imagery. We find that GLOFRIS simulates inundation extent in urban areas as well as it simulates inundation extent elsewhere. We also used both the GLOFRIS and benchmark inundation maps to simulate flood impacts (potential maximum damage). We find that the percentage differences in maximum potential damage using the GLOFRIS and benchmark inundation maps is much lower than the differences in EAD caused by the use of different flood protection standards, and the use of different GCMs, RCPs, and SSPs. We have already shown the overall conclusions to be robust to the latter assumptions.

In future studies, it would be useful to carry out full uncertainty assessments across multiple models such as the multi-modelling exercises carried out for the Inter-Sectoral Impact Model Intercomparison Project (ISIMIP). The value of multi-model studies has been shown at European scale using high-resolution ensembles from Regional Climate Models[21]. As higher-resolution global climate data become available, and the number of global flood inundation models increases, our framework could be used to provide multi-model assessments of adaptation benefits and costs. Indeed, the framework

can be used with inputs from different models, and model parameters can be adjusted based on local knowledge from users.

Increased structural flood protection appears economically attractive in large parts of the world. In some regions, implementing protection standards that maximize NPV can negate absolute increases in risk that would otherwise occur. However, we also show where structural protection can be economically unviable. In those regions, more attention is required for other flood risk management strategies[5]. In practice, feasibility of flood protection is related not only to the economic parameters used here. Other factors that may render structural defences infeasible include: the presence of humans and livelihood activities, soil subsidence, or reduced sediment accretion; or non-economic factors related to structural defences such as loss of existing amenities, tourism, ecosystems, and fisheries. Also, the construction of structural flood protection measures can lead to lock-in and the so-called levee effect[22]. Optimal risk reduction strategies are therefore usually a mix of different measures[12]. Future studies should consider costs and benefits of multiple adaptation strategies, such as retention areas, flood-proofing buildings, early warning systems[23], building codes[12], and post-disaster support. Whilst we limit our analyses to built infrastructure, green measures can also reduce flood risk[24]. In some regions, green measures already provide some flood protection. Information on multiple strategies is essential for integrating disaster risk management into broader development policy discussions, in which trade-offs must be made between risk reduction and other issues, such as health and education. This is particularly the case in low-income countries, where financial resources struggle to satisfy needs[25]. On the other hand, in many regions floods disproportionately affect poor people[25], so risk reduction is commensurate with overall development goals. The current study considers only direct economic damages, whilst floods can also cause extensive indirect damages[26], fatalities, and injury[27]. Methods are required to integrate these into global-scale risk assessments, since these impacts also influence flood protection effectiveness.

Our framework can be used to highlight potential savings through strategies to increase structural flood protection at the sub-national scale. When moving towards implementation of individual measures, detailed studies should be performed using local models and data[9,28], but global analyses help to initiate dialogue with stakeholders and identify priority regions. To increase accessibility to the risk community, results of this study will be integrated into the Aqueduct Global Flood Analyzer webtool (www.wri.org/floods).

Methods

Methods, including statements of data availability and any associated accession codes and references, are available in the online version of this paper.

Received 31 March 2017; accepted 22 June 2017; published online 31 July 2017

References

1. Munich, Re *NatCatSERVICE Database* (Munich Reinsurance Company, Geo Risks Research, 2013).
2. Hirabayashi, Y. *et al*. Global flood risk under climate change. *Nat. Clim. Change* **3,** 816–821 (2013).
3. Winsemius, *et al*. Global drivers of future river flood risk. *Nat. Clim. Change* **6,** 381–385 (2016).
4. Arnell, N. W. & Gosling, S. N. The impacts of climate change on river flood risk at the global scale. *Climatic Change* **134,** 387–401 (2014).
5. Jongman, B. *et al*. Declining vulnerability to river floods and the global benefits of adaptation. *Proc. Natl Acad. Sci. USA* **112,** E2271–E2280 (2015).
6. Ward, P. J. *et al*. Assessing flood risk at the global scale: Model setup, results, and sensitivity. *Environ. Res. Lett.* **8,** 044019 (2013).
7. Winsemius, H. C. *et al*. A framework for global river flood risk assessments. *Hydrol. Earth Syst. Sci.* **17,** 1871–1892 (2013).
8. UNISDR *Global Assessment Report on Disaster Risk Reduction. Making Development Sustainable: The Future of Disaster Risk Management* (United Nations International Strategy for Disaster Reduction Secretariat, 2015).
9. Ward, P. J. *et al*. Usefulness and limitations of global flood risk models. *Nat. Clim. Change* **5,** 712–715 (2015).
10. *Towards a World of Cities in 2050. An Outlook on Water-Related Challenges* (Netherlands Environmental Assessment Agency PBL, 2014).
11. Sadoff, C. W. *et al*. *Securing Water, Sustaining Growth: Report of the GWP/OECD Task Force on Water Security and Sustainable Growth* (Univ. Oxford, 2015).
12. Aerts, J. C. J. H. *et al*. Evaluating flood resilience strategies for coastal megacities. *Science* **344,** 473–475 (2014).
13. Kind, J. M. Economically efficient flood protection standards for the Netherlands. *J. Flood Risk Manag.* **7,** 103–117 (2014).
14. Kull, D., Mechler, R. & Hochrainer-Stigler, S. Probabilistic cost-benefit analysis of disaster risk management in a development context. *Disasters* **37,** 374–400 (2013).
15. Scussolini, P. *et al*. FLOPROS: an evolving global database of flood protection standards. *Nat. Hazard Earth Sys.* **16,** 1049–1061 (2016).
16. VanVuuren, D. P. *et al*. The representative concentration pathways: an overview. *Climatic Change* **109,** 5–31 (2011).
17. O'Neill, B. C. *et al*. A new scenario framework for Climate Change Research: the concept of shared socioeconomic pathways. *Climatic Change* **122,** 387–400 (2014).
18. Sperna Weiland, F. C., Van Beek, L. P. H., Kwadijk, J. C. J. & Bierkens, M. F. P. Global patterns of change in discharge regimes for 2100. *Hydrol. Earth Syst. Sci.* **16,** 1047–1062 (2012).
19. Sampson, C. C. *et al*. A high-resolution global flood hazard model. *Wat. Resour. Res.* **51,** 7358–7381 (2015).
20. Trigg, M. A. *et al*. The credibility challenge for global fluvial flood risk analysis. *Environ. Res. Lett.* **11,** 094014 (2016).
21. Alfieri, L., Feyen, L., Dottori, F. & Bianchi, A. Ensemble flood risk assessment in Europe under high end climate scenarios. *Glob. Environ. Change* **35,** 199–212 (2015).
22. Di Baldassarre, *et al*. Socio-hydrology: conceptualising human-flood interactions. *Hydrol. Earth Syst. Sci.* **17,** 3295–3303 (2013).
23. Pappenberger, F. *et al*. The monetary benefit of early flood warnings in Europe. *Environ. Sci. Policy* **51,** 278–291 (2015).
24. Van Wesenbeeck, B. K., de Boer, W., Narayan, S., van der Star, W. R. L. & de Vries, M. B. Coastal and riverine ecosystems as adaptive flood defences under a changing climate. *Mitig. Adapt. Strateg. Glob. Change* http://dx.doi.org/10.1007/s11027-016-9714-z (2016).
25. Hallegatte, *et al*. *Shock Waves: Managing the Impacts of Climate Change on Poverty* (World Bank, 2016).
26. Koks, *et al*. Integrated direct and indirect flood risk modeling: development and sensitivity analysis. *Risk Anal.* **35,** 882–900 (2015).
27. Jonkman, S. N., Vrijling, J. K. & Vouwenvelder, A. C.W. M. Methods for the estimation of loss of life due to floods: a literature review and a proposal for a new method. *Nat. Hazards* **46,** 353–389 (2008).
28. Jonkman, S. N. Advanced flood risk analysis required. *Nat. Clim. Change* **3,** 1004 (2013).

Acknowledgements

The research leading to these results received funding from the Netherlands Organisation for Scientific Research (NWO) in the form of a VIDI grant (grant no. 016.161.324) and the Aqueduct Global Flood Analyzer project, via subsidy 5000002722 from the Netherlands Ministry of Infrastructure and the Environment. The latter project is convened by the World Resources Institute. J.C.J.H.A. and W.J.W.B. received additional funding from the NWO in the form of VICI and VIDI Grants (grant no. 453.14.006 and 452.14.005). We thank O. Wing and M. Trigg for providing benchmarking inundation maps.

Author contributions

All authors conceived and designed the experiments and contributed to discussions on, and writing of, the paper. P.J.W., B.J., P.S. and H.C.W. performed the experiments. P.J.W., A.D.L., P.S. and H.C.W. analysed the data. P.D.B. contributed to the benchmarking exercise.

Additional information

Supplementary information is available in the online version of the paper. Reprints and permissions information is available online at www.nature.com/reprints. Publisher's note: Springer Nature remains neutral with regard to jurisdictional claims in published maps and institutional affiliations. Correspondence and requests for materials should be addressed to P.J.W.

Competing financial interests

The authors declare no competing financial interests.

Methods

We developed a method to assess the benefits and costs of reducing future river-flood risk (expressed as expected annual damage, EAD, in urban areas) at the sub-national scale, by increasing flood protection standards offered by dykes. Here, urban refers to all kinds of built-up areas and artificial surfaces. Sub-national scale is defined as the next administrative unit below national scale in the Global Administrative Areas Database (GADM). We used the method to assess the benefits and costs of three adaptation objectives: maximizing NPV of the investment (optimize); keeping future EAD constant in absolute terms (constant absolute risk); and keeping future EAD as a percentage of GDP constant (constant relative risk). In brief, benefits of increasing structural protection are defined as the difference between: future EAD if dykes remain constant at assumed current height and future EAD if the height of dykes is increased. Since we do not have global projections of subsidence, this factor is not included. Costs are defined as the sum of investment and capitalized maintenance costs. The different steps are described in the following paragraphs.

Calculation of EAD. Urban damage was calculated at sub-national scale using GLOFRIS[6,7] for several return periods (2, 5, 10, 25, 50, 100, 250, 500, and 1,000 years), and EAD was calculated as the integral of the area under an exceedance probability–damage curve (risk curve) across these different return periods. Validation of GLOFRIS in past studies, and further benchmarking for this study, are described in Supplementary Information 3. To account for flood protection standards, the risk curve was truncated for return periods lower than or equal to the protection standard. For example, if a sub-national unit is assumed to have a flood protection standard of 25 years, damages associated with floods up to and including that return period were set to zero prior to integration. For return periods exceeding the protection standard, it is assumed that flood protection does not affect the flood extent. For each future simulation (that is, each combination of 1 GCM, 1 RCP, and 1 SSP), EAD was calculated under future (2080) and current (1960) conditions, and the factor difference between these was calculated. This factor was then applied to the EAD estimate based on the current data to estimate bias-corrected future EAD. Current protection standards were taken from the modelled layer of the FLOPROS data set[15]. FLOPROS provides modelled protection standards at the sub-national scale. These modelled protection standards have been validated against actual flood protection standards in place in several regions in ref. 15. Sensitivity to this assumption is assessed by re-running the analyses assuming: current flood protection to be: half that stated in the FLOPROS database; and double that stated in the FLOPROS database (Supplementary Information 2.5). Since flood inundation is not simulated hydrodynamically, the framework does not account for the transfer of risk from better-protected upstream areas to downstream areas.

To calculate the urban damage for the individual return periods, we used the GLOFRIS model[6,7]. The GLOFRIS setup and input data used to carry out the damage simulations used for the current and future periods in this study are described in detail in ref. 3. We refer the reader to these papers for details of this model and the setup used in the current paper; here, we provide a brief overview for the sake of clarity. In essence, the cascade involves the following four processes: hydrological and hydraulic modelling to develop daily time series of flood volumes; extreme value statistics to estimate flood volumes for different return periods; inundation modelling for different return periods; and impact modelling.

Hydrological and hydraulic modelling to develop daily time series of flood volumes: Daily gridded discharge and flood volumes were simulated ($0.5^\circ \times 0.5^\circ$) using PCR-GLOBWB-DynRout[29], which requires daily gridded meteorological input data (precipitation, temperature, global radiation). Validation is described in refs 6,29,30. For current climate conditions, EU-WATCH forcing data[31] were used for the period 1960–1999. For future climate conditions, the forcing data were daily bias-corrected outputs[32] from the following Global Climate Models (GCMs): HadGEM2-ES, IPSL-CM5A-LR, MIROC-ESM-CHEM, GFDL-ESM2M, and NorESM1-M. For each GCM, daily gridded discharge and flood volumes were simulated for the (model) periods 1960–1999 and 2060–2099 (represent climate conditions in 2080).

Extreme value statistics: From each of the daily gridded flood volume time series, annual hydrological year time series of maximum flood volumes were extracted, using the approach described in ref. 6. Then, we fit a Gumbel distribution through these time series, based on non-zero data, and used the resulting Gumbel parameters per grid cell to estimate flood volumes for the following return periods (2, 5, 10, 25, 50, 100, 250, 500, and 1,000 years), conditioned to years in which zero flood volumes were exceeded. This produces coarse resolution ($0.5^\circ \times 0.5^\circ$) maps of flood volume for each return period.

Inundation modelling: The coarse resolution flood volume maps were then converted into high-resolution ($30'' \times 30''$) inundation maps using the inundation downscaling module of GLOFRIS[7]. This model was used because it is the only global flood hazard model of those assessed in a recent comparison study[20] that simulates high-resolution inundation under future climate scenarios. The models compared in that study are: CaMa-Flood[33], JRC[34], ECMWF[35], SSBN-Bristol[19], CIMA-UNEP[8], and GLOFRIS. The CaMa-Flood model has been used to examine changes in flood risk for several future scenarios[2]. However, due to the large computational time requirement, they only simulated the fraction of inundation per $2.5' \times 2.5'$ cell, a much lower resolution than GLOFRIS, and not including flood depths. The JRC model has been used to assess future changes in flood risk[36]. However, they only used inundation maps at $30'' \times 30''$ (that is, the same as GLOFRIS) based on current climate. They then used a low-resolution global hydrological model ($0.5^\circ \times 0.5^\circ$) to simulate changes in discharge in the future. They did not simulate future inundation, but used changes in future discharge to adjust the probability of flooding in the future. This approach was specifically chosen to 'optimize the trade-off between information content and computing resources needed'. To the best of our knowledge, the ECMWF model has not been used to assess inundation for future scenarios. The SSBN-Bristol and CIMA-UNEP models use information from regional flood frequency analysis to derive flood hydrographs. They are not directly forced by climate input data, and therefore their current setup does not allow for future climate change studies.

GLOFRIS employs a volume-spreading algorithm, rather than a hydrodynamic modelling scheme. Whilst it may be preferable to use more complex hydrodynamic models if the aim of the study is to simulate present-day inundation as accurately as possible, when carrying out a scenario modelling exercise such as the one carried out for this paper, an important consideration is whether the model provides reasonable performance but also produces inundation maps within a reasonable time frame and for an acceptable computational cost. In the case of this study, the important consideration is whether the model can simulate inundation with high enough skill so that the flood impact results do not deviate excessively from impact results based on a higher-resolution benchmark data set. We have tested this extensively, as discussed in Supplementary Information 3.2.3.

Impact modelling: Each high-resolution inundation map was combined with gridded socio-economic data, also at a horizontal resolution of $30'' \times 30''$, to calculate urban damage per grid cell, and these data were then aggregated to the sub-national scale. In GLOFRIS, urban damage is calculated using the inundation maps to represent hazard, a map of asset values in urban areas to represent exposure, and a depth-damage function to represent vulnerability[6]. The asset value map is based on a percentage urban area per grid cell multiplied by an estimate of urban asset values per square kilometre. Data for current urban area per grid cell were taken from the HYDE database[37], and data for current urban asset values were taken from ref. 6. In the HYDE data set, and therefore in this study, urban refers to all kinds of built-up areas and artificial surfaces. Future changes in urban densities and asset values were taken from ref. 3, and were computed using gridded population and GDP data from the GISMO/IMAGE model[38,39], using the method described in ref. 40. For the future scenarios of GDP and population, data were used from the Shared Socioeconomic Pathway (SSP) database[17]. The spatial resolution of the exposure data is the same as the spatial resolution of the hazard data, so they are commensurate for impact assessment. Validation of the urban damage values has been carried out for several countries in past studies[6,41].

Estimation of benefits. Benefits were calculated as the difference between future EAD with and without additional flood management investments. First, we estimated EAD assuming that no additional investment takes place in the future compared to current. Effectively, this means that existing dykes are maintained at their current height. We then estimated, per sub-national unit, the protection standard required in 2080 (under different combinations of RCP/SSP) to achieve the 'optimize', 'constant absolute risk', and 'constant relative risk' objectives. The maximum protection standard is capped at 1,000 years, since this is the largest return period for which damages are physically simulated in GLOFRIS.

Estimation of costs. Costs are calculated by summing investment and capitalized maintenance costs. All costs reported in this paper are in US$2005 at Purchasing Power Parity (PPP), and were adjusted from the original values stated in the literature using GDP deflators from the World Bank, and annual average market exchange rates between Euros and US$ taken from the European Central Bank. The cost estimates described below are in constant US$, and are adjusted to PPP values in the model (using World Bank converters), since the benefits derived from GLOFRIS are also in PPP values.

First, we estimate the investment costs of dykes in the USA. Cost estimates in the literature vary widely, as shown in several recent overview papers[42–44]. To account for this variation, here we applied three cost estimates: high, middle, and low. For the middle-estimate investment costs, we use a value of US$ 7.0 million km m^{-1} heightening. This estimate is based on reported costs in New Orleans in ref. 45. It pertains to all investments costs, including ground work, construction, and engineering costs, property or land acquisition, environmental compensation, and project management. We selected this value since it also is in the middle of other recent estimates in refs 42,43 from the USA and the Netherlands. Moreover, it is close to the average cost of heightening reported in ref. 46 of US$ 6.6 million km m^{-1} heightening, for 21 dyke-rings in the

Netherlands; US$ 6.7 million km m^{-1} heightening for 36 dyke-reaches in Canada reported in ref. 44; and US$ 8.4 million km m^{-1} heightening for coastal dykes in the Netherlands reported in ref. 44. In a recent study based on empirical investment cost data from the Netherlands and Canada, ref. 44 found that investment costs per metre heightening are well described by a linear function without intercept. They conclude that for large-scale studies it is sufficient to assume linear costs for each metre of heightening, including the initial costs, and therefore we assumed this to be the case for the current study. These cost estimates were then adjusted for all other countries by applying construction index multipliers[47] (based on civil engineering construction costs) to account for differences in construction costs across countries[48]. The empirical investigation of dyke costs in ref. 44 also found that the spread in cost estimates caused by factors other than dyke length and height can be well represented by assuming low- and high-cost estimates of $3x$ and $x/3$, where x represents the best cost estimate. Therefore, we also used this approach to carry out our benefit:cost analyses for a low-cost estimate (US$ 2.3 million km m^{-1} heightening) and for a high-cost estimate (US$ 21.0 million km m^{-1} heightening). We assumed maintenance costs to be 1% per year of investment costs[43].

We estimated the kilometre length of dykes required by combining the river network map and the map of urban areas used in GLOFRIS (both $30'' \times 30''$). We calculated the length of rivers of Strahler order 6 or higher (since these are the rivers for which inundation is simulated in GLOFRIS) flowing through urban areas (that is, areas that are indicated as urban in the HYDE database).

To calculate the costs of dyke heightening, an estimate is also required of the (increase in) dyke height needed for each future scenario to facilitate protection against floods for various magnitudes and associated return periods. For each $0.5^\circ \times 0.5^\circ$ grid cell, we estimated the required height of the dyke for a given return period of protection by converting the discharge occurring with the return period into a flow depth. For a given scenario and protection level, and for a given grid cell, we established the heights of the dykes as follows. First we retrieve the discharge occurring with the return period associated with the required protection level from a Gumbel distribution of discharges, established from GLOFRIS as described in ref. 6. Dykes are usually not built directly at the banks of the river, but at a certain distance from the banks within the floodplain. We have here assumed that they are built at a distance of one times the channel width from the river banks. The width and bankfull depth of the channel are taken from the hydrological model PCRGLOB-WB (part of GLOFRIS framework), using:

$$Q = hB\frac{1}{n}R^{2/3}\sqrt{i} \quad (1)$$

where Q is the discharge [L^3 T^{-1}], h is the flow depth [L], B is the flow width [L], n is the Manning roughness [T L$^{-1/3}$], R is the hydraulic radius [L] (equal to $hB/(2h+B)$) and i is the slope of the channel [−]. In large rivers, flow depth is much smaller than the flow width, and R can be approximated by h, reducing equation (1) into:

$$Q = B\frac{1}{n}h^{5/3}\sqrt{i} \quad (2)$$

In our case, a part of the flow is through the main channel and part over the part of the floodplain that lies in between the dykes, both having different dimensions and roughness values. We therefore split up equation (2) into a channel part and a floodplain part as follows:

$$Q = \left[B_c\frac{1}{n_c}h^{5/3} + B_f\frac{1}{n_f}(h-h_{bf})^{5/3}\right]\sqrt{i} \quad (3)$$

where c and f are channel and floodplain respectively, and h_{bf} is the bankfull channel depth [L]. We solve this equation for h. The required height of the dyke is then $h - h_{bf}$.

Cost–benefit analysis. To carry out the cost–benefit analysis, several assumptions are required. Firstly, the discount rate; we used a real discount rate of 5% per year, and performed sensitivity analysis using 3% and 8% per year Secondly, we assumed the protection level increases linearly between 2020 and 2050, and that by 2050 dykes are designed to the standard required for the climate at the end of the twenty-first century (2060–2099). The flows of costs and benefits are discounted until 2100.

Data availability. The data that support the findings of this study are available from the corresponding author upon request. The costs and benefits per sub-national unit are available within the article (and its supplementary information files) for all RCP/SSP combinations; each individual GCM; different discount rates; high, middle, and low cost estimates; and different assumptions on assumed baseline protection.

References

29. Van Beek, L. P. H., Wada, Y. & Bierkens, M. F. P. Global monthly water stress: I. Water balance and water availability. *Wat. Resour. Res.* **47,** W07517 (2011).
30. Wada, Y., Van Beek, L. P. H. & Bierkens, M. F. P. Nonsustainable groundwater sustaining irrigation: A global assessment. *Wat. Resour. Res.* **48,** W00L06 (2012).
31. Weedon, G. P. *et al*. Creation of the WATCH Forcing Data and its use to assess global and regional reference crop evaporation over land during the twentieth century. *J. Hydrometeorol.* **12,** 823–848 (2011).
32. Hempel, S., Frieler, K., Warszawski, L., Schewe, J. & Piontek, F. A trend-preserving bias correction - the ISI-MIP approach. *Earth Syst. Dynam.* **4,** 219–236 (2013).
33. Yamazaki, D., Kanae, S., Kim, H. & Oki, T. A physically based description of floodplain inundation dynamics in a global river routing model. *Wat. Resour. Res.* **47,** W04501 (2011).
34. Dottori, F. *et al*. Development and evaluation of a framework for global flood hazard mapping. *Adv. Wat. Res.* **94,** 87–102 (2016).
35. Pappenberger, F., Dutra, E., Wetterhall, F. & Cloke, H. L. Deriving global flood hazard maps of fluvial floods through a physical model cascade. *Hydrol. Earth Syst. Sci.* **16,** 4143–4156 (2012).
36. Alfieri, L. *et al*. Global projections of river flood risk in a warmer world. *Earth's Future* **5,** 171–182 (2017).
37. Klein Goldewijk, K., Beusen, A., Van Drecht, G. & De Vos, M. The HYDE 3.1 spatially explicit database of human-induced global land-use change over the past 12,000 years. *Glob. Ecol. Biogeogr.* **20,** 73–86 (2011).
38. Van Vuuren, D. P., Lucas, P. L. & Hilderink, H. Downscaling drivers of global environmental change: enabling use of global SRES scenarios at the national and grid levels. *Glob. Environ. Change* **17,** 114130 (2007).
39. Bouwman, A. F., Kram, T. & Klein Goldewijk, K. *Integrated Modelling of Global Environmental Change. An Overview of IMAGE 2.4* (PBL Netherlands Environmental Assessment Agency, 2006).
40. Jongman, B., Ward, P. J. & Aerts, J. C.J. H. Global exposure to river and coastal flooding: long term trends and changes. *Glob. Environ. Change* **22,** 823–835 (2012).
41. Ward, P. J. *et al*. Strong influence of El Niño Southern Oscillation on flood risk around the world. *Proc. Natl Acad. Sci. USA* **111,** 15659–15644 (2014).
42. Aerts, J. C. J. H., Botzen, W. & De Moel, H. Cost estimates of flood protection and resilience measures. *Ann. New York Acad. Sci.* **1294,** 39–51 (2013).
43. Jonkman, S. N., Hillen, M. M., Nicholls, R. J., Kanning, W. & Van Ledden, M. Costs of adapting coastal defences to sea-level rise—New estimates and their implications. *J. Coast. Res.* **29,** 1212–1226 (2013).
44. Lenk, S., Rybski, D., Heidrich, O., Dawson, R. J. & Kropp, J. P. Costs of sea dikes—regressions and uncertainty estimates. *Nat. Hazard. Earth Sys.* **17,** 765–779 (2017).
45. Bos, A. J. *Optimal Safety Level for the New Orleans East Polder. A Preliminary Risk Analysis* (VU University Amsterdam, 2008).
46. De Grave, P. & Baarse, G. *Kosten van maatregelen. Informatie ten behoeve van het project Waterveiligheid 21e eeuw* (Deltares, 2011).
47. *The 2009 Global Construction Cost and Reference Yearbook* (Compass International Consultants, 2009).
48. Ward, *et al*. Partial costs of global climate change adaptation for the supply of raw industrial and municipal water: a methodology and application. *Environ. Res. Lett.* **5,** 044011 (2010).